Photochromic Bis(thiophen-3-yl)maleimides Studied with Time-Resolved Spectroscopy

C. Elsner,[†] T. Cordes,[†] P. Dietrich,[‡] M. Zastrow,[‡] T. T. Herzog,[†] K. Rück-Braun,[‡] and W. Zinth*,[†]

Munich Center for Integrated Protein Science, CIPSM, and Lehrstuhl für BioMolekulare Optik, Department Physik, Ludwig-Maximilians-Universität München, Oettingenstrasse 67, D-80538 München, Germany, and Institut für Chemie, Technische Universität Berlin, Strasse des 17. Juni 135, D-10623, Berlin, Germany

Received: August 4, 2008; Revised Manuscript Received: November 24, 2008

The dynamics of the ring-closure reaction of three different bis(thiophen-3-yl)maleimides are investigated using ultrafast spectroscopy in the visible range. The structures of the molecules differ with respect to substitution of the thiophene ring and the maleimide. The experiments reveal reaction kinetics which point to the population of an excited electronic state for several nanoseconds. In the case of completely unsubstituted thiophene rings, a long excited-state lifetime (biexponential decay with 3 and 15 ns) can be observed. The remaining ultrafast absorption transients of this molecule are due to relaxational processes on the excited electronic potential energy surface. The ring-closure reaction has a small yield (<1%) and does not show up in the ultrafast absorption experiments. A dimethyl substitution of the thiophene ring results in completely different behavior: after transients related to relaxation in the excited electronic state, one finds pronounced absorption transients with $\tau = 16$ ps which represent the partial decay of the excited electronic state and the formation of the ring-closed isomer. Another fraction of the emitting excited electronic state decays again on the few nanosecond time scale. The experiments suggest that the open isomer of the dimethyl-substituted imides exists in two conformations.

1. Introduction

Photochromic compounds have received special attention due to their potential applications for optical data storage and optical switching[1−3] and the possibilities for investigating the ultrafast reaction processes in real time.[4] The most common photochromic systems are linked to elementary chemical reactions, e.g., pericyclic reactions[4] or *Z*/*E*-isomerizations:[2,5] here, several compounds based on azobenzene,[6,7] fulgides/fulgimides[8−11] and hemithioindigos[5,12−14] or other diarylethenes[1] may serve as photochromic centers. The impressive progress has brought up new compounds,[15] with high thermal stability of the involved isomers, strongly separated absorption bands, and thermally irreversible photoreactions with high photochemical quantum yields.[1] In this respect Irie and co-workers developed the class of diarylethenes (DAE) featuring heterocyclic rings.[1,16−21] These compounds undergo light-induced ring-opening and ring-closure reactions where cyclohexadiene (CHD) and hexatriene (HT) parts are interconverted (Scheme 1). The structures of the closed (*C*) and open (*O*) isomers of the investigated DAE compounds are displayed in Scheme 1. A major advantage of DAE molecules is that the different isomers show good stability.[1,22] Some DAE molecules may even undergo more than 10^4 photochromic cycles without decomposition,[2] and some compounds yet keep their photochromic behavior in the crystalline form.[23] These properties are the prerequisite for a promising application of DAE molecules as switches in material science.[6,12,24]

These interesting properties of DAE motivated the present investigation of the ring-closure reaction of special DAE derivatives based on maleimides structure. The bis(thiophen-3-yl)maleimides show several advantages compared with other DAEs: the absorption maxima undergo a bathochromic shift in comparison with perfluorated compounds.[1] It is also known that maleimides are more resistant to hydrolysis reactions than anhydrides.[1] These properties are important for biological applications. Furthermore, a direct functionalization of the DAE switching unit via the imide nitrogen is possible. The photochemical reactions and the photochromic performance are characterized by steady-state and time-resolved spectroscopy in the visible spectral range. We present results on three DAE compounds (see Scheme 1) which show differences in fluorescence and photochemical reactivity. The ultrafast response of the photoexcited open form *O* is investigated and analyzed. These results allow one to deduce reaction schemes where the time constants of each reaction step and the differences in

SCHEME 1: Upper Part Shows the Structure of the Investigated DAE Compounds 1−3; Lower Part Details the Pericyclic Reactions of the Different Molecules

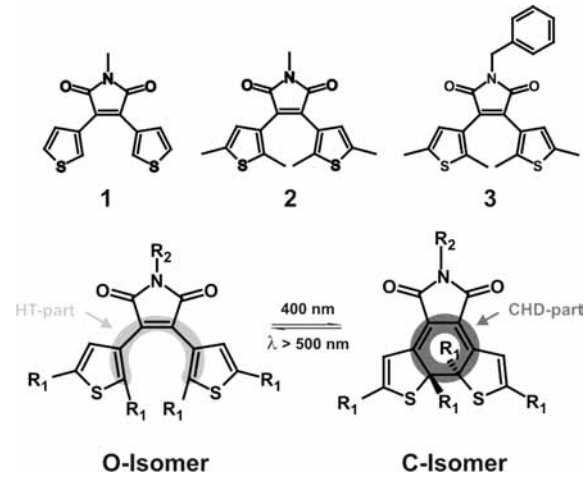

* To whom correspondence should be addressed.
[†] Ludwig-Maximilians-Universität München.
[‡] Technische Universität Berlin.

10.1021/jp806945m CCC: $40.75
Published on Web 01/14/2009

reaction yield are explained by the molecular structure and the steric interactions.

2. Materials and Methods

2.1. Materials and CW Spectroscopy. The synthesis of the bis(thiophen-3-yl)maleimides (Scheme 1, **1**−**3**) is described in the Supporting Information. The pure *O*-isomers of compounds **1**−**3** were dissolved in acetonitrile (Sigma, purity 99.8%). The composition of the sample depends on the applied illumination: thereby the differences of the absorption spectra of the two isomers (see below) allows one to convert any mixture of the two isomers by extended exposure to visible light at long wavelengths (λ > 490 nm) completely back to the *O*-isomer. For this purpose a cold light source, type KLC2500 filtered by a 3 mm thick GG495, both from Schott, Mainz, was used in the experiments. This illumination was used to maintain a high concentration of the *O*-isomers (>95%) during the femtosecond experiments. For compounds **2** and **3**, a photostationary state (PSS400) containing both isomers, the closed *C*-isomer and the *O*-isomer, was prepared by illumination with a mercury−xenon lamp (Hamamatsu, filtered by a 3 mm thick long-pass filter GG385 (Schott) leading to an illumination spectrum with peaks at 400−430 nm). PSS400 contained approximately 70% of the *C*-isomer and 30% of the *O*-isomer. The specific *O*/*C* ratio for compounds **2** and **3** varied slightly.

The stationary UV−vis absorption spectra were recorded using a spectrophotometer (Perkin-Elmer, Lambda19). In these experiments a concentration of ∼0.05 mM was used. For the determination of the reaction quantum yield concerning the *O* → *C* isomerization process, we recorded the absorbance change of the *C*-isomer absorption after illumination with defined amount of energy at 414 nm. The setup and the procedure to obtain the quantum yield was described recently in ref 12. (Observation wavelength 500 nm in a range with exclusive *C* absorption, illumination by a laser module at 414 nm with a power of 0.3 mW (VLMA-1, Roithner.) The induced absorption change was recorded after different illumination periods. The quantum efficiency Φ_{PC} was calculated from the number of photons absorbed by the *O*-isomers after extrapolation to zero illumination, from the recorded changes in the concentration of the *C*-isomer (determined with a value of the extinction coefficient of the *C*-isomer of $\varepsilon^{C}_{(500)} = 4800\ M^{-1}\ cm^{-1}$). Fluorescence spectra, corrected for the spectral sensitivity of the apparatus, were measured with a fluorimeter (Spex, Fluorolog 1680). The fluorescence quantum yield Φ_{Fl} was determined using the dye coumarin 153 dissolved in ethanol as a reference dye. A value for the fluorescence quantum yield of coumarin 153 in ethanol of $\Phi_{Fl} = 0.38$[25] was used.

2.2. Time-Resolved Spectroscopy.

2.2.1. Femtosecond Pump−Probe. A home-built chirped pulse laser amplifier system (CPA) was employed for the time-resolved experiments (for details see refs 6, 12, and 13). The CPA delivered pulses at a central wavelength of 804 nm with a duration of 90 fs, a pulse energy of 0.6 mJ, and a repetition rate of 1 kHz. For the excitation of the *O*-isomer the laser fundamental was frequency-doubled in a BBO crystal (type I) to 402 nm. The excitation energy of the ∼100 fs pulses for the pump−probe experiment was adjusted to be in the range of 150−400 nJ. A small part of the fundamental generated the white light continuum used as probe light.[26] Pump-induced absorption changes in the different sample solutions were recorded by a multichannel detection setup.[27] The probing process covered a spectral range from 340 to 650 nm. The polarization of pump and probe beam at the sample location

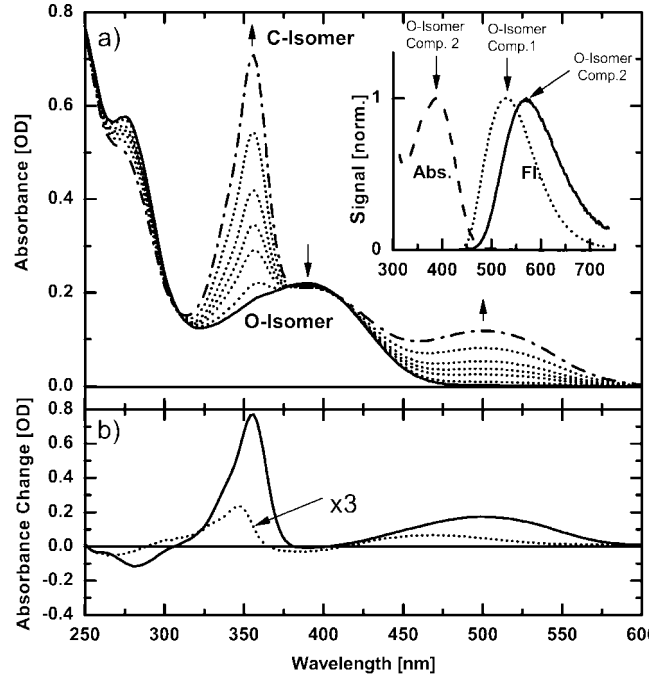

Figure 1. (a) UV−vis absorption spectra (compound **2**) of the open form (*O*-isomer, solid line) and at the photostationary state PSS400 (dash dotted line) by irradiation with 400 nm light. Illumination times: 0, 4, 15, 25, 40, 70, and 125 s (dotted lines). The inset shows the absorption spectrum of compound **2** and the fluorescence spectra of the *O*-isomers of compounds **1** and **2**. (b) Difference spectra between the photostationary state PSS400 and the *O*-isomer (compound **2**, solid line), compound **1** (dotted line) after irradiation with 400 nm light and irradiation with 530 nm.

was at magic angle (54.7°). The sample solution (kept in a fused-silica flow cell with an optical path length of 0.5 mm) had a millimolar concentration leading to an optical density of the sample at the excitation wavelength of ∼1 OD. The beam diameter of the pump light in the sample was ∼150 μm, providing a homogeneous excitation density over the area of the probe pulse (diameter of ∼60−80 μm). A mechanical chopper blocked every second excitation pulse to improve referencing. During the transient absorption measurement the different sample solutions were pumped through the fused-silica flow cell using a peristaltic pump with Teflon tubing exchanging the sample volume in the laser focus completely between two consecutive pump pulses. Continuous illumination at long wavelengths (see above) maintained a high concentration of the *O*-isomer during the femtosecond experiments.

The data points at certain delay times between pump and probe pulses were recorded with repetitive scans (ca. 5−15) which were averaged. Each data point from one single scan is averaged over 1000 laser shots. Transient background signals from the pure solvent (acetonitrile) were recorded and subtracted (after appropriate weighting) from the sample signal. The error of the recorded absorbance change was smaller than 0.3 mOD for delay times t_D > 0.5 ps. The GVD and corresponding time-zero dispersion were calculated from the material dispersions using a Sellmeier fit. The time-dependent absorbance difference spectra are plotted in Figures 2 and 3 as a function of delay time. Please note that a linear scale is used around time zero and a logarithmic one is used for later delay times. The recorded data was simulated according to a rate equation model, where the time constants were derived by a global least-squares fitting algorithm (Levenberg−Marquart).[28,29]

2.2.2. Nanosecond Experiments. A home-built spectrometer was used for the determination of the fluorescence lifetimes of

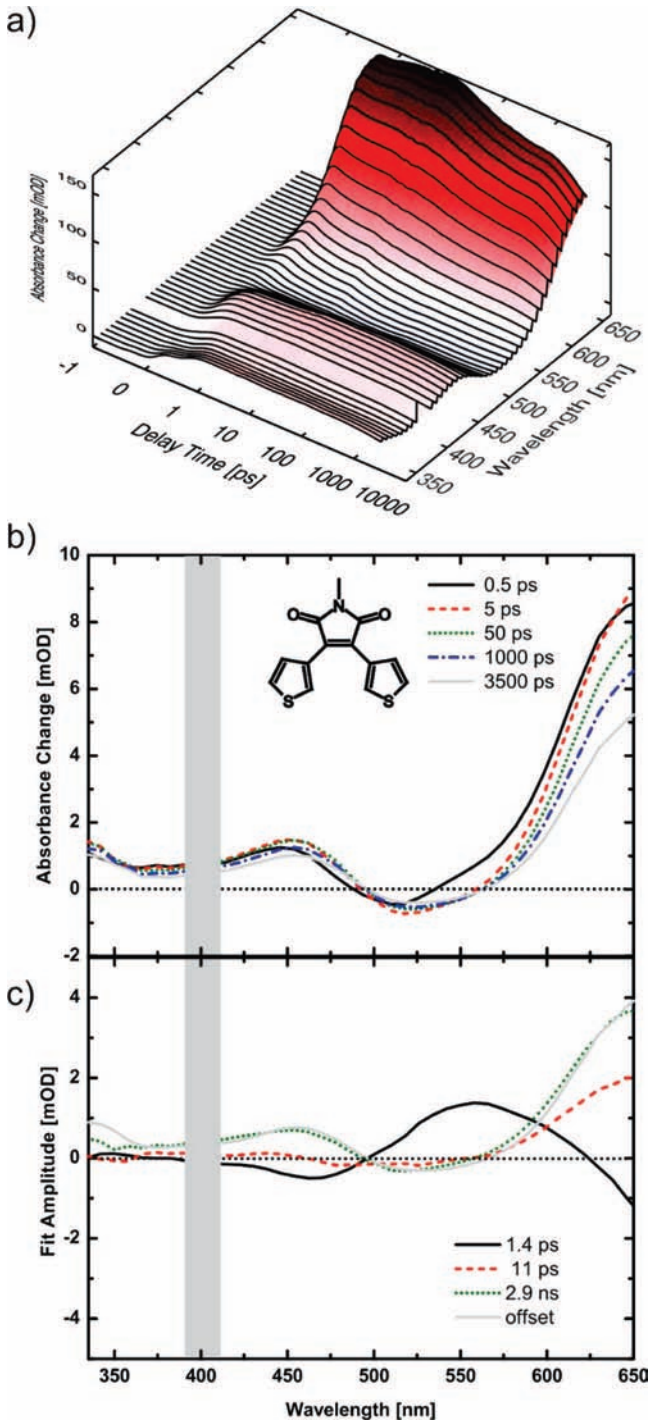

Figure 2. (a) Three-dimensional plot of the transient absorption changes vs delay time and probing wavelength of compound **1**. A linear time scale is used for the delay times $t_D < 1$ ps, and a logarithmic scale is used thereafter. (b) Transient spectra at certain delay times; (c) amplitude spectra (DAS) derived from a global fitting routine for the ring-closing process. The amplitude indicated as offset may describe mainly the changes related with the 15 ns final decay of the excited electronic state.

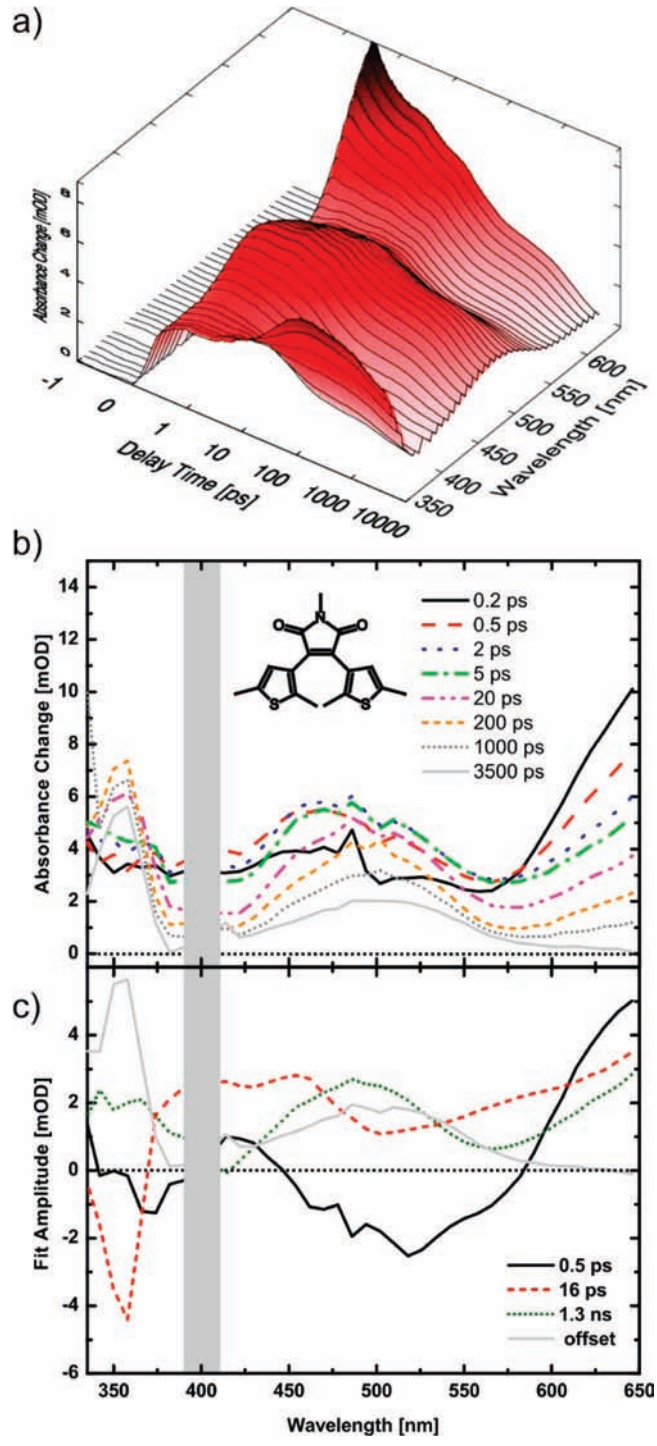

Figure 3. (a) Three-dimensional plot of the transient absorption changes vs delay time and probing wavelength of compound **2**. (A linear time scale is used for the delay times $t_D < 1$ ps, and a logarithmic scale is used thereafter.) (b) Transient spectra at certain delay times; (c) amplitude spectra (DAS) derived from a global fitting routine for the ring-closing process.

the compounds. The sample was excited with a pulsed Nd:YAG (third harmonic, 355 nm) at a repetition rate of 40 Hz. The emission (at 630 nm) of the samples was collected using objectives and recorded by a photodiode (Thorlabs DET10A/M) and an oscilloscope (Tektronix TCS 320D). A temporal resolution of the setup of ~8 ns could be achieved.

3. Results

3.1. CW Characterization. The investigated DAE compounds can exist in two photoisomeric forms as shown in the lower part of Scheme 1. The open form (*O*-isomer) shows a characteristic HT part. It may undergo a photoinduced ring-closure reaction forming the *C*-isomer with the central CHD part. In all three compounds (**1**−**3**), the central double bond of the HT part is included in a maleimide moiety, whereas the remaining double bonds are part of heteroaromatic substituents,

TABLE 1: Spectroscopic Data of All Investigated Compounds 1−3[a]

	stationary data					time-resolved data			
	peak positions			quantum yields		time constants			
	Abs (*O*)/nm	Abs (*C*)/nm		Fl (*O*)/nm	$\Phi_{PC}(O\rightarrow C)$/%	$\Phi_{Fl}(O)$/%	τ_1/ps	τ_2/ps	τ_3/ns	τ_4/ns
1	386			531		29.0	1.4	11	2.9	15[b]
2	392	356	500	569	22 ± 5	0.4	0.5	16	1.3	
3	392	356	500	573	20 ± 5	0.3	0.4	17	0.9	

[a] The left part of the table (stationary data) gives the wavelength of the absorption peak of both isomers (Abs) and the fluorescence peak of the *O*-isomer (Fl), the photochemical quantum yield for the $O \rightarrow C$ process $\Phi_{PC}(O\rightarrow C)$, and the fluorescence quantum yield $\Phi_{Fl}(O)$ of the *O*-isomer. The right part of the table summarizes the time constants for the time-resolved data of the respective compound derived from a global fitting routine. [b] Derived from nanosecond experiments.

e.g., thiophene or 2,5-dimethylthiophene. The absorption spectra of the *O*-isomers of all three compounds are very similar. They display a broad absorption band around 390 nm (presumably due to the $S_0 \rightarrow S_1$ transition) and a second band at 275 nm (for compound **2** see Figure 1a). Compounds **2** and **3** show a pronounced photochromic behavior. When these compounds are illuminated into the S_1 band (400/430 nm), the spectra of the samples are strongly altered (dotted curves in Figure 1a and difference spectrum (solid line) in Figure 1b for compound **2**)—two new absorption bands arise at 355 and 500 nm. The new absorption bands characterize the formation of the *C*-isomer. It has to be noted that the integrated oscillator strength of the DAE molecules increases considerably upon formation of the *C*-isomer. The absorption band ($S_0 \rightarrow S_1$ transition) of the *C*-isomer is strongly red-shifted with respect to the *O*-isomer. This fact points to a more planar and strongly conjugated π-electron system in the *C*-isomer. In addition, the planar geometry of the closed isomer is supposed to have less conformational freedom with respect to the open conformer. When the *C*-isomers of compounds **2** and **3** are illuminated in the long-wavelength band at $\lambda > 490$ nm the absorption changes induced by the 400 nm illumination are reversed. There is a complete reconversion of the molecules into the open form. The photochromism of compound **1** is less pronounced. Illumination (400 nm) into the S_1 band induces spectral changes which have some similarities with the ones found for compounds **2** and **3**. There is induced absorption at 350 nm and >400 nm which point to the formation of the *C*-isomer. However, the amplitudes of the absorption changes are much weaker and suggest that the formation of the *C*-isomer is much less efficient for compound **1** than for compounds **2** and **3** (see Figure 1b, dotted curve). For more information see the Supporting Information. The normalized fluorescence spectra of the *O*-isomer of compounds **1** and **2** ($\lambda_{exc} = 400$ nm) are shown in the inset in Figure 1a. The two emission spectra differ in their position and have considerably different quantum yields (see Table 1). One finds that the emission of compound **1** peaks around ∼525 nm, whereas compound **2** peaks at 570 nm. Both positions correspond to large Stokes shifts of ∼7000 and ∼9000 cm^{-1}, respectively. These values are in a range found previously for related compounds.[30,31] The fluorescence quantum yields of the *O*-isomers of compounds **2** and **3** are found to be 0.4% and 0.3%, respectively (Table 1). The photochemical quantum yield for the ring-closure reaction of both compounds is around 20%. For compound **1** a different behavior is found: a much larger fluorescence quantum yield of 29% and a small photochemical quantum yield (<1%) is observed. The characteristic absorption and emission properties of all molecules are summarized in Table 1.

3.2. Time-Resolved Measurements. The photophysical and photochemical reaction dynamics initiated by near-UV light at 400 nm were investigated for all three compounds in their open form by means of transient absorption spectroscopy. The ultrafast absorption changes during the first 3.5 ns for compounds **1** and **2** are shown in Figures 2 and 3, respectively.

***3.2.1. Compound* 1.** Optical excitation of molecule **1** (Figure 2, parts a and b, $\lambda_{exc} = 402$ nm) leads to a rapid absorption increase due to excited-state absorption (ESA) within 0.5 ps. The observed ESA extends throughout the whole investigated spectral range. Modulations in the induced absorption spectrum may be related to ground-state bleaching (GSB, 380 nm) close to the excitation wavelength and to stimulated emission (SE) around 505 nm. This assignment is possible by comparing the femtosecond data with stationary data shown in Figure 1. Here, the absorption maximum of the *O*-isomer is found at 390 nm, whereas the fluorescence peaks at 520 nm. SE leads to a weak negative absorption signal in this wavelength range. Within the next picoseconds the features assigned to SE shift to longer wavelengths and finally settle at 520 nm after ∼5 ps; this spectral position is in good agreement with stationary data. Only small further changes in the signal amplitude are observed on the picosecond time scale. The decay of the induced absorption due to ESA and the reduction of SE occur on a time scale of several nanoseconds. Even at the end of our observation period (3.5 ns), the absorption change is not completely recovered. Emission experiments on the nanosecond time scale show that the final decay of the excited electronic state occurs with a time constant of 15 ns. A global fitting procedure of the absorption changes, including all data points starting from $t_D = -1$ ps to 3.5 ns, allows describing the temporal behavior with four exponentials and related time constants of $\tau_1 = 1.4$ ps, $\tau_2 = 11$ ps, $\tau_3 = 2.9$ ns, and the additional 15 ns process from the nanosecond experiments. The decay-associated spectra (DAS of compound **1**) related to the time constants $\tau_1-\tau_3$ are shown in Figure 2c. The spectral characteristics of the DAS of τ_1 and τ_2 allow one to assign these processes to motions of the molecule on the excited-state potential surface. No significant hints for ground-state return (e.g., decay of SE, bleach recovery) can be found on the fast time scales. These fast absorption dynamics are hence most likely related to relaxation, solvation, and conformational rearrangement processes after photoexcitation. It is not until the nanosecond time scale that ESA and SE are reduced and that most of the molecules return to their ground state. The different DAS do not show distinct features at the wavelength positions, where the stationary illumination experiments revealed absorption changes (see dotted curve in Figure 1b). Therefore, it remains uncertain if any one of the picosecond processes is related to the formation of the closed form as a photoproduct.

***3.2.2. Compound* 2.** The overview of the transient absorption changes of compound **2** (see Figure 3, parts a and b) reveals a behavior which differs considerably from that of compound **1**. In both data sets there is unstructured absorption over a broad spectral range at early delay times (Figure 3, $t_D = 0.2$ ps). The

signal at later delay times (t_D < 20 ps) shows that ESA with a maximum at long wavelengths >650 nm is again superimposed by SE at 550 nm and a weak GSB close to the excitation wavelength. This assignment is reasonable as the local minima found in the induced absorption at a delay time $t_D = 0.5$ ps (Figure 3) are found at the spectral region of ground-state absorption and fluorescence (compare with Figure 1). In contrast to compound **1**, the spectral signatures are drastically changed just within several hundred femtoseconds: in this early time regime, a distinct and broad absorption band appears between 430 and 530 nm and the features due to SE are red-shifted up to 575 nm. Simultaneously, ESA at wavelength >600 nm is reduced, while the signal at shorter wavelength (<400 nm) remains nearly constant within this period. On the time scale of 5−20 ps the absorption difference spectrum again changes considerably: now there is a significant increase of a narrow absorption band around 350 nm while the signal related to ESA (450 nm) decays by about 50%. At longer delay times (>100 ps) the absorption signal gradually approaches a spectral shape which is similar to the stationary difference spectrum found in the CW experiments (Figure 1b). This feature can hence be assigned to the newly formed *C*-isomer. A global fitting procedure with three exponentials allows one to describe the observed kinetics. Three time constants $\tau_1 = 0.5$ ps, $\tau_2 = 16$ ps, $\tau_3 = 1.3$ ns together with a constant offset are necessary to reproduce the experimental data (Figure 3c). The DAS of the time constant $\tau_1 = 0.5$ ps shows an increase in absorption in the spectral range between 450 and 570 nm and a decrease at wavelengths >570 nm. We associate this spectral signature to motions on the excited-state potential surface and to related relaxation and solvation processes. The negative amplitude of the 0.5 ps DAS around 500 nm could point to a red-shift of SE, to a change in ESA, or to the rapid formation of a photoproduct. Two arguments can exclude a subpicosecond formation of the *C*-isomer: there is (i) no increase in absorption in the range of the strong *C*-isomer absorption band around 350 nm and (ii) no simultaneous reduction of the SE signature in the long-wavelength region. On the time scale of τ_1 the SE is not decreasing, but its spectrum is shifted. The DAS related with time constant $\tau_2 = 16$ ps shows features expected for *C*-isomer formation: a broad decay of induced absorption at λ_{probe} > 375 nm and a strong increase of a narrow absorption band around 350 nm. The spectral signatures at long wavelengths point to a partial decay of the ESA. At late time delays, toward the end of the observation window, strong absorption changes occur with a time constant $\tau_3 = 1.3$ ns. The related DAS indicates that this process is again related to the decay of the excited electronic state, since its features involve the decay of ESA bands at >600 nm and ∼500 nm together with the disappearance of GSB around 400 nm. However, there is no indication for the formation of a 350 nm band with this time constant. At the end of our observation time the absorption difference spectrum closely resembles the stationary absorption difference spectrum.

The time-resolved absorption data of compound **3** are very similar to those of compound **2**: the data sets appear to be nearly identical, and just the time constants found in the global analysis are slightly different. The global fitting routine results in three time constants $\tau_1 = 0.4$ ps, $\tau_2 = 17$ ps, $\tau_3 = 0.9$ ns. The DAS corresponding to these time constants exhibit the same spectral shape as found for the related DAS of compound **2** (Figure 3c).

We may summarize our results as follows: after optical excitation all compounds display transients with time constants in the range of ∼1 ps, ∼10−20 ps, and 1−3 ns. Compound **1** shows no significant product formation on the picosecond time scale. These observations are in good agreement with the small changes in the absorption spectrum upon CW illumination. On the other hand, a strongly fluorescent state (quantum yield of 29% for the open form) with a lifetime in the nanosecond range is found. The transient data do not allow to assign the product formation process of compound **1** to a specific time constant. Compounds **2** and **3** show completely different absorption dynamics. After initial relaxational processes on the subpicosecond time scale, product formation and a related excited-state decay are observed within ∼10−20 ps. However, a considerable fraction of the molecules remains in the excited electronic state at that time. The final decay of these trapped molecules occurs within a few nanoseconds back to the ground state of the original *O*-isomer and not to the product *C*-form.

4. Discussion

The experimental investigations could show that substitutions of the DAE molecules influence both the reaction dynamics and the photochemical quantum yields.

(i) Substitution of the maleimide: Only minor changes were observed when the maleimide is substituted by a methyl or a benzyl group (compound **2** vs **3**). The absorption spectra remain almost unchanged, the quantum yields for the ring-closing reaction are nearly unaffected, and the final decay of the excited electronic state is weakly decelerated (1.3 vs 0.9 ns). The overall behavior of the compounds **2** and **3** is hence nearly identical.

(ii) Substitution of the thiophene part: A strong change of the reaction parameters is found upon the methylation in the 2- and 5-position of the thiophene rings: the unmethylated sample, compound **1**, shows a long-lived (∼15 ns) and strongly fluorescent ($\Phi_{Fl} = 29\%$) excited electronic state S_1. The yield of the ring-closure reaction is small (<1%) as seen from steady-state and time-resolved experiments. Extended illumination in the 400 nm range leads to irreversible changes of the sample. In contrast, the two methyl-substituted compounds **2** and **3** exhibit absorption transients, pointing to the formation of the *C*-isomer with a time constant of ca. 16 ps. The yield of product formation is in the range of 20% for compounds **2** and **3**. Surprisingly, the transient data sets of both compounds also show a nanosecond component with the spectral signature of an excited electronic state.

The results for the various compounds can be interpreted by consideration of the structural restrictions imposed by methylation of the thiophene rings. For the open form of the DAE molecules the methyl groups lead, in case of a planar arrangement of the two thiophene rings, to strong steric repulsion. These steric interactions are responsible for a heterogeneity of the sample in the electronic ground state, which is already known from other DAE systems.[32] The samples of compounds **2** and **3** may hence be divided into two types of open conformers: a parallel (p) and an antiparallel (ap) configuration. This behavior is already known from other DAE derivatives.[1,31−34] The parallel conformation prohibits the DAE molecules to undergo the light-induced ring-closure reaction. On the other hand, the antiparallel arrangement of the thiophene rings leads to a geometry where conrotatory motions over small angles allow it to perform the ring-closure reaction. This behavior has been discussed in the literature:[32−34] here, the photochemical quantum yield was improved by specific substitution stabilizing the antiparallel arrangement. We will show below that the same arguments allow us to explain the observed behavior of the investigated compounds.

In Figure 4 we present a schematic reaction model in order to discuss the experimental observations on a molecular level.

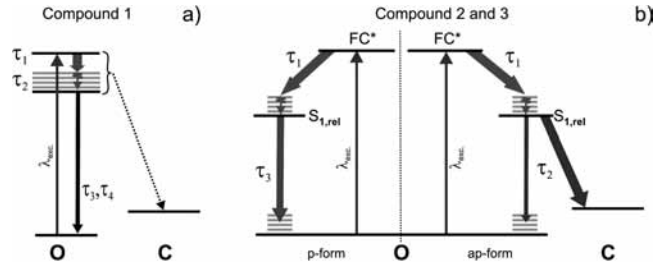

Figure 4. (a) State model for the DAE compound **1**. (b) State model for the DAE *O*/*C* photoisomerization of the investigated DAE **2** and **3** (p-form, parallel form; ap-form, antiparallel form).

4.1. The Photoactive Species (Figure 4b). A sample containing the two different conformers of the *O*-isomer is excited by light at 400 nm to the corresponding Franck−Condon (FC) states. Fast initial relaxational processes occur—as in many other photochromic molecules—on the time scale of 1 ps. During this reaction, rearrangement processes of the molecules and the surrounding solvent occur together with initial vibrational relaxation. For molecules in the reactive antiparallel arrangement of the thiophene rings, the changes in the electronic structure, due to the excitation process, lead to conrotatory motions which guide the system toward the geometry suitable for ring closure. In compounds **2** and **3** the ring closure is completed with the $\tau_2 = 16$ ps transient. This interpretation is supported by the shape of the DAS which reflects both the decay of ESA and the formation of product absorption with the 16 ps process. Product formation is evident for the absorption rise of a narrow band of the closed form at 355 nm (see Figure 1). Molecules with the inactive parallel arrangement of the thiophene rings stay in a relaxed S_1 state and return to the ground state of the open form via internal conversion and only to minor extent via radiative processes (time constant τ_3). The inspection of DAS in the long-wavelength range, where ESA dominates the signal, shows similar amplitudes for the τ_2 and the τ_3 processes. We may conclude that both channels are followed by approximately 50% of the molecules. The weak fluorescence emission ($\Phi_{Fl} \cong 0.4\%$) of compounds **2** and **3** mainly originates from the relaxed S_1 state. Since the lifetime of the S_1 state is much longer in the nonreactive than in the reactive channel, this stationary fluorescence emission is dominated by the nonreactive molecules. Taking a radiative lifetime of ∼50 ns (deduced from compound **1** where $\Phi_{Fl} = 29\%$ and the excited-state lifetime is $\tau_4 = 15$ ns) and a lifetime of the S_1 state of 1 ns with a 50% occupation of the inactive species, we estimate a fluorescence quantum efficiency of 0.5% which is in the range of the experimentally found values (see Table 1).

Even if the analysis of the experimental data based on the assumption of a heterogeneous sample with two ground-state conformers seems very convincing, we cannot rule out alternative explanations. For example, the experimental results can also be interpreted with a model containing only one ground-state conformer: in this case the simultaneous presence of the photoproduct and the S_1 state of the educt on the 100 ps time scale would require an early branching of the reaction in the S_1 state. After branching, the two channels would guide the system to completely different regions of the conformational space of the excited electronic state where one region leads within 16 ps to the fast ring closure, whereas the other one brings the system back to the ground state of the open form on the 1 ns time scale.

4.2. The Nonphotoactive Species (Figure 4a). For compound **1** the situation is completely different. The reduced steric restrictions of compound **1** allow the molecules to access a wide conformational space. There are no pronounced energetic barriers which may guide a considerable fraction of the molecules into the vicinity of the reactive conformation. As a consequence the majority of the molecules excited to the Franck−Condon region of the excited electronic S_1 state undergo relaxation and solvation processes and vibrational relaxation (∼1, 10 ps) without reaching the reactive area of the potential energy landscape. They finally cross over to the ground state of the open form. Apparently internal conversion is not accelerated by the presence of conical intersections or a narrow gap between the S_1 and S_0 surfaces. The absorption change on the nanosecond time scale indicates that the majority of the molecules undergo internal conversion with $\tau_3 = 3$ ns and $\tau_4 = 15$ ns. The weak absorption increase in the range of the absorption band of the *C*-isomer around 350 nm (see Figure 1b) gives some indication for product formation with a small quantum yield.

5. Conclusions

In conclusion, we have investigated three newly synthesized DAE molecules with different substituents on the maleimide part and thiophene rings. Whereas a substitution of the central imide did not influence reaction dynamics and reaction yields, the methylation of the thiophene rings strongly modulates the molecular properties. The presence of the methyl groups at both rings seems to keep a considerable fraction of the DAE ground-state molecules in a geometry with antiparallel arrangement of the thiophene rings. The ring-closure reaction occurs on the time scale of several picoseconds with a photochemical quantum yield of ∼20%. It is surprising that the ring-closing reaction is completed before the spectral signatures of the excited electronic state vanish. This points to the coexistence with a second molecular species, where the steric interactions prohibit a photoinduced ring-closure reaction. In the absence of the methyl groups the reaction quantum yield is strongly reduced, and the lifetime of the S_1 state is in the range of nanoseconds. This indicates that the relaxation of the steric interaction allows the system to access a wide region of conformational space from where ring closure cannot occur.

Acknowledgment. This work was supported by the Deutsche Forschungsgemeinschaft through the DFG-Cluster of Excellence Munich-Centre for Advanced Photonics and the SFB 749.

Supporting Information Available: Details of synthesis and sample characterization and UV−vis absorption spectra of the open form of compound **1**. This material is available free of charge via the Internet at http://pubs.acs.org.

References and Notes

(1) Irie, M. *Chem. Rev.* **2000**, *100*, 1685.
(2) Feringa, B. *Molecular Switches*; Wiley-VCH: Weinheim, Germany, 2001.
(3) Dürr, H., Bouas-Laurent, H., Eds. *Photochromism: Molecules and Systems*; Elsevier: Amsterdam, The Netherlands, 2003.
(4) Miyasaka, H.; Arai, S.; Tabata, A.; Nobuto, T.; Mataga, N.; Irie, M. *Chem. Phys. Lett.* **1994**, *230*, 249.
(5) Cordes, T.; Schadendorf, T.; Priewisch, B.; Rück-Braun, K.; Zinth, W. *J. Phys. Chem. A* **2008**, *112*, 581.
(6) Spörlein, S.; Carstens, H.; Satzger, H.; Renner, C.; Behrendt, R.; Moroder, L.; Tavan, P.; Zinth, W.; Wachtveitl, J. *Proc. Natl. Acad. Sci. U.S.A.* **2002**, *99*, 7998.
(7) Koller, F. O.; Sobotta, C.; Schrader, T. E.; Cordes, T.; Schreier, W. J.; Sieg, A.; Gilch, P. *Chem. Phys.* **2007**, *341*, 258.
(8) Koller, F. O.; Schreier, W. J.; Schrader, T. E.; Malkmus, S.; Schulz, C.; Dietrich, S.; Rück-Braun, K.; Braun, M. *J. Phys. Chem. A* **2008**, *112*, 210.

(9) Malkmus, S.; Koller, F. O.; Draxler, S.; Schrader, T. E.; Schreier, W. J.; Brust, T.; DiGirolamo, J. A.; Lees, W. J.; Zinth, W.; Braun, M. *Chem. Phys. Lett.* **2006**, *417*, 266.

(10) Koller, F. O.; Schreier, W. J.; Schrader, T. E.; Sieg, A.; Malkmus, S.; Schulz, C.; Dietrich, S.; Rück-Braun, K.; Zinth, W.; Braun, M. *J. Phys. Chem. A* **2006**, *110*, 12769.

(11) Malkmus, S.; Koller, F. O.; Heinz, B.; Schreier, W. J.; Schrader, T. E.; Zinth, W.; Schulz, C.; Dietrich, S.; Rück-Braun, K.; Braun, M. *Chem. Phys. Lett.* **2006**, *417*, 266.

(12) Cordes, T.; Weinrich, D.; Kempa, S.; Riesselmann, K.; Herre, S.; Hoppmann, C.; Rück-Braun, K.; Zinth, W. *Chem. Phys. Lett.* **2006**, *428*, 167.

(13) Cordes, T.; Heinz, B.; Regner, N.; Hoppmann, C.; Schrader, T. E.; Summerer, W.; Rück-Braun, K.; Zinth, W. *; ChemPhysChem* **2007**, *8*, 1713.

(14) Cordes, T.; Schadendorf, T.; Rück-Braun, K.; Zinth, W. *Chem. Phys. Lett.* **2008**, *455*, 197.

(15) Irie, M.; Sakemura, K.; Okinaka, M.; Uchida, K. *J. Org. Chem.* **1995**, *60*, 8305.

(16) Irie, M.; Fukaminato, T.; Sasaki, T.; Tamai, T.; Kawai, T. *Nature* **2002**, *420*, 759.

(17) Higashiguchi, K.; Matsuda, K.; Irie, M. *Angew. Chem., Int. Ed.* **2003**, *42*, 3537.

(18) Matsuda, K.; Irie, M. *J. Photochem. Photobiol., C* **2004**, *5*, 169.

(19) Higashiguchi, K.; Matsuda, K.; Tanifuji, N.; Irie, M. *J. Am. Chem. Soc.* **2005**, *237*, 8922.

(20) Fukaminato, T.; Umemoto, T.; Iwata, Y.; Yokojima, S.; Yoneyama, M.; Nakamura, S.; Irie, M. *J. Am. Chem. Soc.* **2007**, *129*, 5932.

(21) Kobatake, S.; Takami, S.; Muto, H.; Ishikawa, T.; Irie, M. *Nature* **2007**, *446*, 778.

(22) Irie, M.; Uchida, K. *Bull. Chem. Soc. Jpn.* **1998**, *71*, 985.

(23) Abe, S.; Uchida, K.; Yamazaki, I.; Irie, M. *Langmuir* **1997**, *13*, 5504.

(24) Schrader, T. E.; Schreier, W. J.; Cordes, T.; Koller, F. O.; Babitzki, G.; Denschlag, R.; Renner, C.; Dong, S. L.; Löweneck, M.; Moroder, L.; Tavan, P.; Zinth, W. *Proc. Natl. Acad. Sci. U.S.A.* **2007**, *104*, 15729.

(25) Jones, G.; Bergmark, W. R. *J. Phys. Chem.* **1985**, *89*, 295.

(26) Huber, R.; Satzger, H.; Zinth, W.; Wachtveitl, J. *Opt. Commun.* **2001**, *194*, 443.

(27) Seel, M.; Wildermuth, E.; Zinth, W. *Meas. Sci. Technol.* **1997**, *8*, 449.

(28) Satzger, H.; Root, C.; Gilch, P.; Zinth, W.; Wildemann, D.; Fischer, G. *J. Phys. Chem. B* **2005**, *109*, 4770.

(29) Holzwarth, A. R. Data Analysis of Time-Resolved Measurements. In *Biophysical Techniques in Photosynthesis*; Amesz, J., Hoff, A. J., Eds.; Kluwer: Dordrecht, The Netherlands, 1996.

(30) Miyasaka, H.; Araki, S.; Tabata, A.; Nobuto, T.; Mataga, N.; Irie, M. *Chem. Phys. Lett.* **1994**, *230*, 249.

(31) Tamai, N.; Miyasaka, H. *Chem. Rev.* **2000**, *100*, 1875.

(32) Miyasaka, H.; Nobuto, T.; Murakami, M.; Itaya, A.; Tamai, N.; Irie, M. *J. Phys. Chem. A* **2002**, *106*, 8096.

(33) Okabe, C.; Nakabayashi, T.; Bobuyuki, N.; Fukaminato, T.; Kawai, T.; Irie, M.; Sekiya, H. *J. Phys. Chem. A* **2003**, *107*, 5384.

(34) Irie, M.; Mohri, M. *J. Org. Chem.* **1988**, *53*, 805.

JP806945M